BMC Cancer

RESEARCH

Open Access

PLCD1 expression for early detection and prognosis in High-Grade serous ovarian cancer

Jue Young Kim[1], Ha-Yeon Shin[1], Razaul Haque[2], Eun-Suk Kang[3] and Jae-Hoon Kim[1*]

Abstract

Background High-grade serous ovarian cancer (HGSOC) is the most common and aggressive subtype of epithelial ovarian cancer, characterized by rapid progression and poor prognosis. Despite advances in treatment, most cases are diagnosed at an advanced stage, and current diagnostic markers such as CA-125 have limited utility for early detection or treatment stratification. This study aimed to investigate the clinical significance and biological Function of phospholipase C delta 1 (PLCD1) in HGSOC.

Methods PLCD1 expression was assessed by immunohistochemistry (IHC) using tissue microarrays (TMA) comprising normal, borderline, and HGSOC tissues. Survival analyses were performed using Kaplan–Meier methods. PLCD1 expression in HGSOC cell lines was evaluated by Western blotting. Functional studies were conducted using PLCD1 knockdown and overexpression cell lines. Cell proliferation, invasion, and 3D spheroid assays were used to assess tumor cell behavior. A xenograft mouse model was used to evaluate the effect of PLCD1 overexpression on tumor growth in vivo.

Results PLCD1 expression was significantly elevated in HGSOC tissues compared to normal and borderline tissues. Low PLCD1 expression was associated with significantly worse overall and disease-free survival in patients with HGSOC ($n = 101$). In vitro, PLCD1 knockdown increased proliferation in OVCA429 cells, while overexpression in OVCAR3 cells suppressed colony formation. In vivo, PLCD1 overexpression significantly reduced tumor growth in a xenograft model.

Conclusion PLCD1 functions as a tumor suppressor in HGSOC and is associated with improved clinical outcomes. These findings suggest that PLCD1 may serve as a prognostic biomarker and potential therapeutic target in ovarian cancer.

Keywords High-grade serous ovarian cancer (HGSOC), PLCD1, Tumor suppressor, Prognosis, Diagnosis, Tissue microarray (TMA), Xenograft model

*Correspondence:
Jae-Hoon Kim
jaehoonkim@yuhs.ac
[1]Department of Obstetrics and Gynecology, Gangnam Severance Hospital, Yonsei University College of Medicine, Seoul, Republic of Korea
[2]School of Medicine, Sungkyunkwan University, Suwon, Gyeonggi-do, Republic of Korea
[3]Department of Laboratory Medicine and Genetics, Samsung Medical Center, Sungkyunkwan University School of Medicine, Seoul, Republic of Korea

Introduction

High-grade serous ovarian cancer (HGSOC) is the most common and aggressive subtype of ovarian cancer, characterized by rapid progression and poor prognosis [1]. It typically originates from the fallopian tubes or surface epithelium of the ovary and frequently metastasizes throughout the peritoneal cavity [2]. Despite advances in treatment, including surgical debulking and platinum-based chemotherapy, most patients eventually experience recurrence, often accompanied by resistance to standard therapies [3]. The molecular complexity of HGSOC, including frequent TP53 mutations and BRCA1/2 gene alterations, contributes to its poor outcomes and presents challenges in clinical management [4].

Understanding the underlying molecular mechanisms of HGSOC is essential for developing effective targeted therapies and improving patient outcomes. However, early detection remains a considerable challenge, as most cases are diagnosed at an advanced stage. Identifying reliable biomarkers for early detection and prognostication is therefore of urgent clinical importance.

Phospholipase C delta 1 (PLCD1) is an enzyme involved in cellular signaling via hydrolysis of phosphatidylinositol 4,5-bisphosphate [5]. In cancer biology, PLCD1 has been implicated in various functions, including the modulation of cell proliferation, migration, and apoptosis [6, 7]. Aberrant expression of PLCD1 has been associated with cancer progression and metastasis in various cancers, including breast and prostate cancers. Recent studies have reported that PLCD1 exerts notable antitumor effects in breast cancer, colorectal cancer, and esophageal squamous cell carcinoma by inhibiting cancer cell proliferation [6, 8, 9]. Additionally, PLCD1 may influence the sensitivity of cancer cells to chemotherapy and radiation. These findings suggest that PLCD1 could serve as a potential biomarker and therapeutic target for personalized cancer treatment.

However, the role of PLCD1 in the pathogenesis and progression of HGSOC remains poorly understood. In this study, we investigated the expression of PLCD1 in high-grade serous ovarian cancer tissues using tissue microarrays (TMA) and analyzed its prognostic value. Furthermore, we explored the functional role of PLCD1 in HGSOC cell lines using in vitro and in vivo models. Our results suggest that PLCD1 acts as a tumor suppressor and may serve as a promising biomarker for HGSOC.

Table 1 Association between PLCD1 expression and clinicopathological features in ovarian TMAs

			PLCD1_Hs_Cy	
Variables	**No.**	**%**	**Mean IHC Score (95% CI)**	**P value**
All	213	100		
Histology				< 0.0001
Normal	68	31.9	38.63 (30.48–46.78)	
Borderline	44	20.7	55.11 (41.05–69.18)	
HGSOC	101	47.4	73.99 (64.50–83.49)	
Age				0.877
< 55	50	49.5	73.24 (58.02–88.47)	
≥ 55	51	50.5	74.73 (62.74–86.72)	
CA125				0.788
Negative	10	9.9	71.55 (43.01–100.08)	
Positive (> 35U/ml)	89	88.1	75.84 (65.62–86.06)	
N.A	2	2.0		
Stage				0.183
I/II	17	16.8	88.2 (66.49–109.91)	
III/IV	84	83.2	71.1 (60.50–81.74)	
Grade				0.464
Moderate	47	46.5	77.8 (62.63–92.92)	
Poor	54	53.5	70.7 (58.39–83.02)	
Chemo response				0.870
Sensitive	78	77.2	74.2 (63.30–85.00)	
Resistant	20	19.8	72.1 (47.86–96.42)	

N.A; Not Available

Histology was analyzed across all TMA tissues; all other variables were assessed in HGSOC cases only ($n = 101$).

Materials and methods

TMAs and patient information

TMAs were obtained from the Korea Gynecologic Cancer Bank of Gangnam Severance Hospital, Yonsei University College of Medicine (No. HTB-P2021-5). All procedures were approved by the Institutional Review Board of Samsung Medical Center (SMC 2019-12-013). The TMAs consisted of 68 normal, 44 borderline, and 101 HGSOC tissues. Clinical information, including treatment and follow-up data, was retrieved from electronic medical records.

Immunohistochemistry staining and scoring

Paraffin-embedded tissue sections were incubated at 65 °C for 20 min, deparaffinized in xylene for 15 min, and rehydrated in graded ethanol (100%, 90%, 70%; 5 min each). Antigen retrieval was performed in 10 mM citrate buffer (pH 6.0) using microwave Heating for 10 min. Endogenous peroxidase was quenched in 3% hydrogen peroxide for 10 min. Sections were then incubated with anti-PLCD1 (ab154610, Abcam) for 2 h at room temperature, followed by EnVision™ Rabbit/Mouse reagent (K5007, Agilent Technologies) for 1 h. Signals were visualized with DAB (K3468, Agilent Technologies) and counterstained with hematoxylin (S3309, Agilent Technologies) for 5 min. PLCD1 expression was semi-quantitatively assessed by multiplying intensity (0–3) and proportion scores (0-100%), yielding a final IHC score (0-300). Patient demographics, clinical characteristics, and IHC results are summarized in Table 1.

Cell culture

YDOV-139, YDOV-157, and YDOV-161 cell lines were established in our laboratory [10–12]. OVCA429, OVCA433, and DOV13 cells were maintained in DMEM (10-013-CV, Corning) supplemented with 10% fetal bovine serum (FBS; 12483-020, Gibco) and 1% penicillin/streptomycin (15140, Gibco). OVCAR3 and SKOV3 were purchased from American Type Culture Collection and maintained according to the supplier's protocol. All cell lines were tested for mycoplasma contamination using the e-Myco™ plus Mycoplasma PCR detection kit (25237, iNtRON Biotechnology).

Protein extraction and Western blotting

Cell lysates were prepared using lysis buffer (9803, Cell Signaling Technology) supplemented with PMSF (8553, Cell Signaling Technology). Protein concentrations were determined by a BCA assay (Sigma-Aldrich). Proteins were separated by SDS-PAGE and transferred onto 0.2 μm nitrocellulose membranes (Pall Corporation). Protein bands were visualized using western blotting luminol reagent (Santa Cruz Biotechnology, Inc.) after incubation with an HRP-conjugated secondary antibody. The primary antibodies used were anti-PLCD1 (ab154610, Abcam), anti-α-actinin (sc-17829, Santa Cruz Biotechnology, Inc.), and anti-β-actin (ab3854, Abcam).

siRNA-mediated knockdown

OVCA429 cells were seeded in 6-well plate and transfected at ~50% confluency with PLCD1 siRNA (5333-3, Bioneer) or control siRNA (SN-1002, Bioneer) using Lipofectamine™ RNAiMAX (13778150, Thermo Scientific) in Opti-MEM (31985-070, Gibco BRL), following the manufacturer's instructions. Knockdown efficiency was assessed 48 h after transfection.

Crystal Violet staining

Cells were seeded in 24-well plates and allowed to adhere overnight. Cells were fixed with 10% acetic acid and 10% methanol, and stained with 0.5% crystal violet (C3886, Sigma-Aldrich) for 1 h. After washing, stained cells were photographed, and dye was solubilized with 1% sodium dodecyl sulfate. Absorbance was measured at 595 nm using a VERSA Max™ microplate reader (Molecular Devices).

Cell invasion assay

Cell invasion was assessed using a 48-well Micro Chemotaxis Chamber (AP48, Neuro Probe). Membranes (PFB8, Neuro Probe) were coated with Matrigel (354234, BD Biosciences) for 1 h. Cells (1×10^5) in serum-free medium were seeded into the upper chambers, and medium containing 10% FBS was placed in the lower chambers. After 24 h, non-invading cells on the upper surface were removed, invaded cells on the lower surface were stained with Differential Quik Stain Kit (38721, Sysmex). Images were captured using an Axio Imager M2 microscope (Carl Zeiss; ×200), and invaded cells were counted in three random fields.

Establishment of stable cell lines

The PLCD1 lentiviral ORF cDNA plasmid with c-GFP tag (pLV-PLCD1-GFPSpark, HG18554-ACGLN) and Control Plasmid (pLV-C-GFPSpark, LVCV-35) were purchased from Sino Biological. HEK293T cells (1×10^6) were co-transfected with 2 μg lentiviral vector, 2 μg packaging plasmids (pCMV delta, pMDG), and Lipofectamin 2000 (Invitrogen). Viral supernatants were collected at 48 and 72 h, and OVCAR3 cells in 24-well plates were infected with 500 μL per well. After 24 h, medium was replaced, and GFP-positive cells were identified by fluorescence microscopy and sorted using FACSAria™ III cell sorter (BD Biosciences).

3D tumor spheroid assay

OVCAR3 stable cells (0.1×10^3 cells) were suspended in a 1:1 mixture of PBS and Matrigel (354234, BD Biosciences), and the mixture was dropped onto a coverslip. After solidification, coverslips were transferred to dishes and overlaid with medium containing 10% FBS. Medium was refreshed every 2 days for up to 9 days. Spheroid morphology was observed with EVOS® FL Cell Imaging System (Life Technologies), and viability was assessed by MTT staining (5 mg/mL, Sigma-Aldrich).

In vivo xenograft tumor model

All animal procedures were approved by the Institutional Animal Care and Use Committee of Yonsei University (Approval No. 2024 – 0266). Six-week-old female BALB/c nude mice (OrientBio Inc.) were anesthetized with alfaxan (76 mg/kg) and xylazine (10 mg/kg). OVCAR3 stable cells (5×10^6) in 1:1 PBS/Matrigel mixture (354234, BD Biosciences) were injected subcutaneously into both flanks. Tumor size was measured with digital calipers, and volume calculated as: volume = length × width^2 × 0.5. After 35 days, tumors were harvested, volume and weight recorded, and tissues fixed in 10% formalin (Sigma-Aldrich).

Public dataset analysis

To validate our findings, we analyzed two independent public cohorts obtained from the Gene Expression Omnibus (GEO): GSE211669 ($n = 126$) [13] and GSE102073 ($n = 85$) [14]. Clinical and survival data were obtained from the supplementary files of each dataset. PLCD1 expression values were extracted from normalized expression matrices provided by GEO. Patients were stratified into high and low expression groups according

to the optimal cutoff values determined by maximally selected rank statistics (log-rank test).

Statistical analysis

Statistical analysis was performed with GraphPad Prism 10.0 (GraphPad Software). Data are presented as mean ± standard deviation (SD). Normality was assessed using Shapiro-Wilk test. Differences between two groups were evaluated using unpaired t-tests or the Mann-Whitney U test. Survival was analyzed by Kaplan–Meier method with log-rank test. P-values < 0.05 were considered significant (* $P < 0.05$, **** $P < 0.0001$).

Results

PLCD1 expression is elevated in HGSOC tissues

We investigated PLCD1 expression by IHC in TMAs comprising normal, borderline tumor, and HGSOC tissues. PLCD1 was strongly expressed in the cytoplasm of epithelial cells, with significantly higher expression observed in HGSOC tissues compared to normal or borderline tissues (Fig. 1A). The mean IHC scores for PLCD1 were 38.63 ± 33.67 in normal tissues, 55.11 ± 46.26 in borderline tumors, and 73.99 ± 48.11 in HGSOC tissues. The difference was statistically significant ($P < 0.0001$), indicating a stepwise increase in PLCD1 expression with disease progression. This pattern suggests that PLCD1 may be involved in malignant transformation.

The clinicopathological characteristics of patients included in the TMA are summarized in Table 1. PLCD1 expression was significantly associated with histologic classification, but not with age, CA125 level, FIGO stage, tumor grade, or chemotherapy response. Although the difference was not statistically significant in Table 1, further stratification revealed that PLCD1 expression tended to be higher in early-stage (I–II) than in advanced-stage (III–IV) tumors ($p = 0.280$; Supplementary Fig. S1A). This pattern indicates that PLCD1 upregulation may occur during the early phases of HGSOC progression, thereby supporting its potential role as an early detection marker.

To evaluate the clinical relevance of PLCD1 expression, we analyzed overall survival (OS) and disease-free survival (DFS) in 101 patients with HGSOC (Fig. 1B). Patients were stratified into high and low PLCD1 expression groups based on the median IHC score. Kaplan–Meier analysis showed that patients in the low PLCD1 expression group had significantly worse OS and DFS than those in the high expression group. For overall survival, the log-rank test yielded $\chi^2 = 4.815$ with a P-value of 0.028. The median OS was 66.00 ± 11.31 months in the low-expression group and 171.00 ± 63.53 months in the high-expression group. The mean OS was 106.26 ± 14.16 months and 159.35 ± 16.50 months, respectively. For disease-free survival, the difference was also statistically significant ($\chi^2 = 4.027$, $P = 0.045$). The median DFS was 21.00 ± 3.41 months in the low-expression group and 39.00 ± 12.90 months in the high-expression group. The mean DFS was 64.61 ± 13.46 months versus 117.02 ± 17.78 months, respectively. These findings further support the prognostic significance of PLCD1 expression, suggesting that reduced PLCD1 levels are associated with shorter survival and more aggressive disease behavior in HGSOC.

To further validate our findings, we analyzed two independent cohorts from public databases GSE211669, $n = 126$; GSE102073, $n = 85$). In GSE211669, patients with low PLCD1 expression had significantly shorter OS compared with those with high PLCD1 expression ($P = 0.048$), and a similar but non-significant trend was observed for progression-free survival (PFS) ($P = 0.112$; Supplementary Fig. S1B). In GSE102073, patients with low PLCD1 also showed a tendency toward shorter OS ($P = 0.051$) and PFS ($P = 0.151$), although the differences did not reach statistical significance (Supplementary Fig. S1C).

PLCD1 regulates HGSOC cell proliferation in vitro

PLCD1 expression in HGSOC cell lines was confirmed by Western blotting, which showed relatively low expression in OVCA429 cells and higher expression in OVCAR3 cells (Fig. 2A). To investigate the functional role of PLCD1, we established both knockdown and overexpression cell lines. For the knockdown model, OVCA429 cells were transfected with PLCD1-targeting siRNA (Fig. 2B). Densitometric analysis of Western blot bands showed that PLCD1 protein levels in siPLCD1-transfected OVCA429 cells were reduced by approximately 63.50% compared to the siControl group.

Colony formation assays showed that PLCD1 knockdown significantly increased the number of colonies. Representative images of the colonies are shown in Fig. 2C. OD quantification demonstrated that the siPLCD1 group had higher absorbance than the siControl group (1.01 vs. 0.69, $P = 0.016$), corresponding to a 1.46-fold increase in cell proliferation (Fig. 2D). However, in the transwell invasion assay, there was no significant difference in invasive capacity between the two groups (Fig. 2E), suggesting that PLCD1 primarily affects proliferation rather than invasion in OVCA429 cells.

For the overexpression model, OVCAR3 cells were transduced with a lentiviral vector carrying PLCD1 or an empty control vector. Stable PLCD1-overexpressing clones were established and verified by Western blotting (Fig. 3A). In 3D spheroid culture assays, PLCD1 overexpression significantly reduced colony number from 103.30 ± 2.52 in the empty vector group to 49.50 ± 5.20 in the PLCD1 group (Fig. 3B, $P < 0.0001$). The spheroids formed by PLCD1-overexpressing cells appeared smaller, more compact, and less proliferative. As with knockdown experiments, invasion assays did not show significant

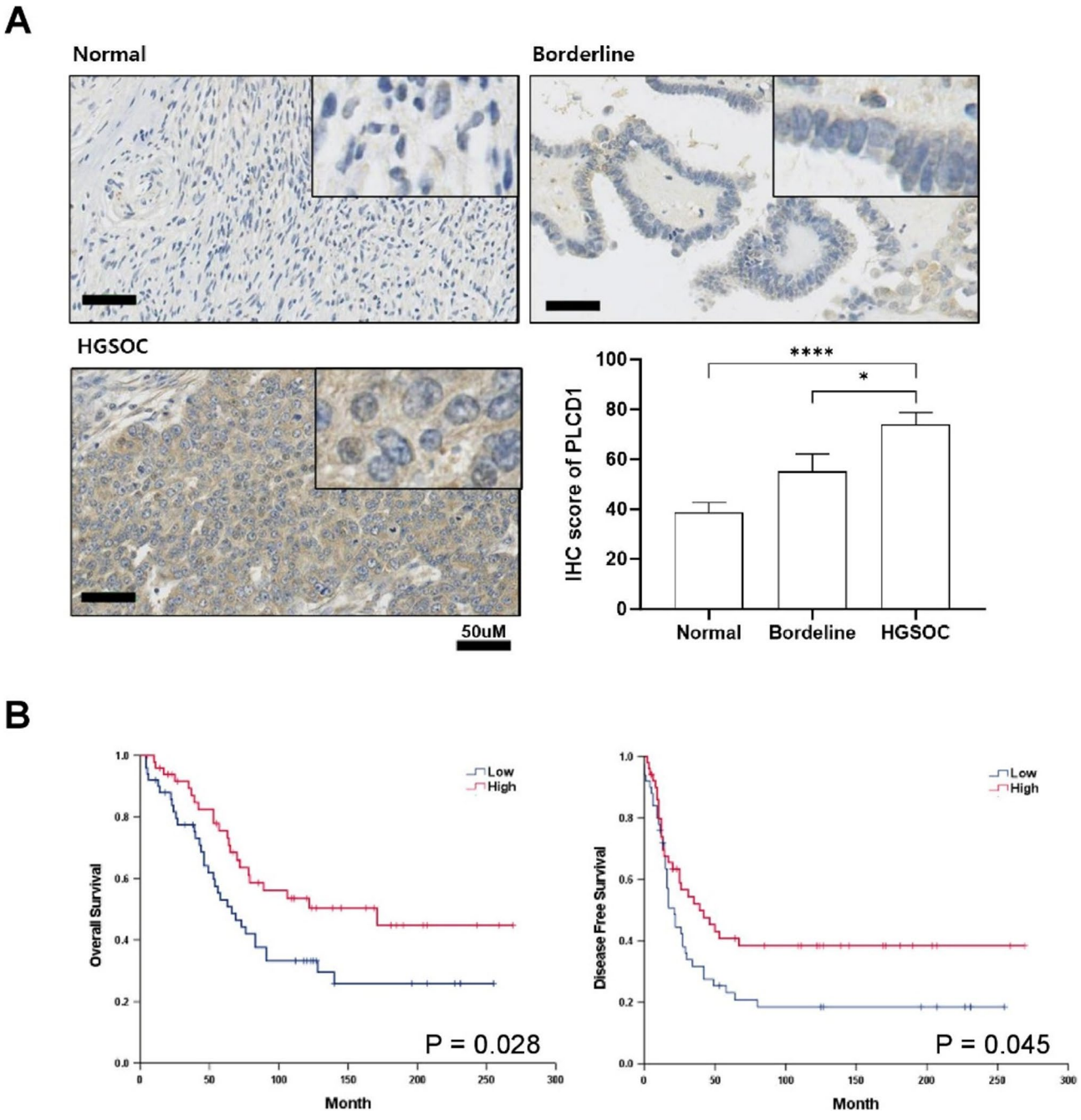

Fig. 1 PLCD1 overexpression was observed in HGSOC tissues. (A) Representative IHC images of PLCD1 expression in normal, borderline, and HGSOC tissues (magnification ×40; scale bar, 50 μm). The mean IHC scores are presented as bar graphs for normal ($n = 68$), borderline ($n = 44$), and HGSOC ($n = 101$) tissues. Statistical significance was determined by unpaired t-test (* $P < 0.05$, **** $P < 0.0001$). (B) Kaplan-Meier survival curves for 101 patients stratified by PLCD1 expression. The curves show differences in OS and DFS between low and high PLCD1 expression groups. Statistical analysis was performed using the log-rank test

differences between the two groups (Fig. 3C). Together, these findings suggest that PLCD1 suppresses cell proliferation in HGSOC cells in vitro.

PLCD1 overexpression reduces tumor growth in vivo

To evaluate whether PLCD1 overexpression affected tumor growth in vivo, we used an OVCAR3-derived xenograft model. OVCAR3 cells were transduced with either PLCD1 or an empty lentiviral vector. The resulting cells were used to establish two groups: the PLCD1 group ($n = 11$) and the Empty group ($n = 4$), which were injected subcutaneously. From 30 day after injection, the tumor growth rate in the PLCD1 group was reduced compared to the Empty group (Fig. 4A). Representative

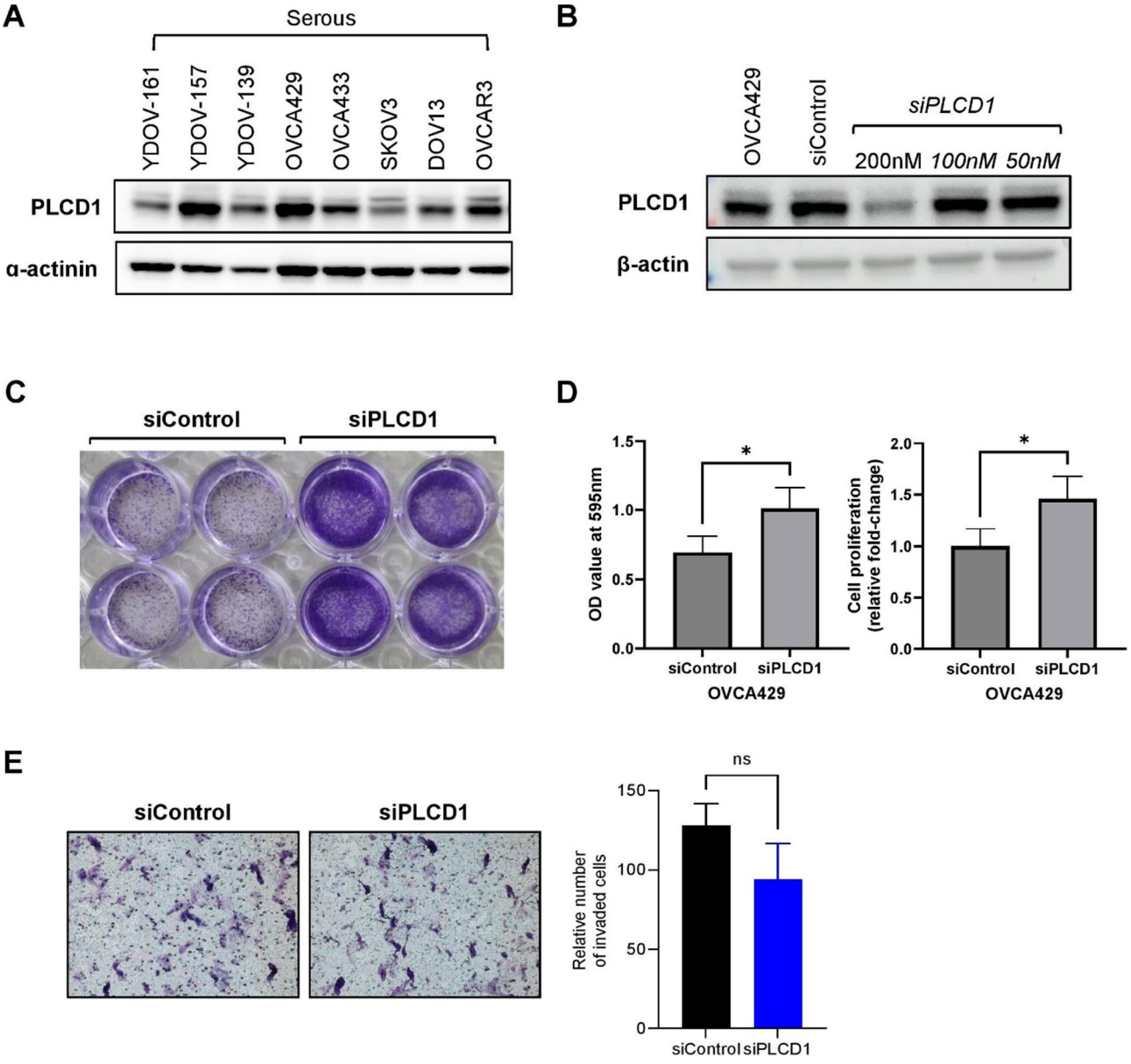

Fig. 2 PLCD1 knockdown enhanced HGSOC cell proliferation in vitro. (A) PLCD1 expression in HGSOC cell lines were measured by Western blotting. α-actinin was used as a loading control. (B) OVCA429 cells were treated with varying concentrations of PLCD1-siRNA (50–200 nM) for 48 h. PLCD1 expression was assessed by Western blotting, with untreated cells (lane 1) and siControl-treated cells (lane 2) included. β-actin was used as a loading control. (C) Colony formation following PLCD1 knockdown in OVCA429 cells. Representative crystal violet-stained images are shown. (D) Quantification of colony formation by absorbance at 595 nm (left) and fold change analysis (right). Data are shown as mean ± SD. Statistical analysis by Mann–Whitney U test ($P < 0.05$). (E) Invasion assay in OVCA429 cells following PLCD1 knockdown. Representative images (left) and quantification of invaded cells (right). Data are shown as mean ± SD (ns: not significant; Mann–Whitney U test)

images of the harvested tumors are shown in Fig. 4B. On day 35, the mean tumor volume in the PLCD1 group was 928.25 ± 335.38 mm^3, compared to 1652.74 ± 715.97 mm^3 in the Empty group, and the difference was statistically significant as determined by the Mann–Whitney U test ($P = 0.037$; Fig. 4C, left). Final tumor weight was also lower in the PLCD1 group (0.69 ± 0.28 g) compared to the Empty group (0.96 ± 0.15 g), although the difference was not statistically significant (Fig. 4C, right). These results suggest that PLCD1 overexpression may suppress tumor growth in vivo.

Discussion

The present findings reveal a potential tumor-suppressive function of PLCD1 in HGSOC, as evidenced by its elevated expression in tumor tissues and its association

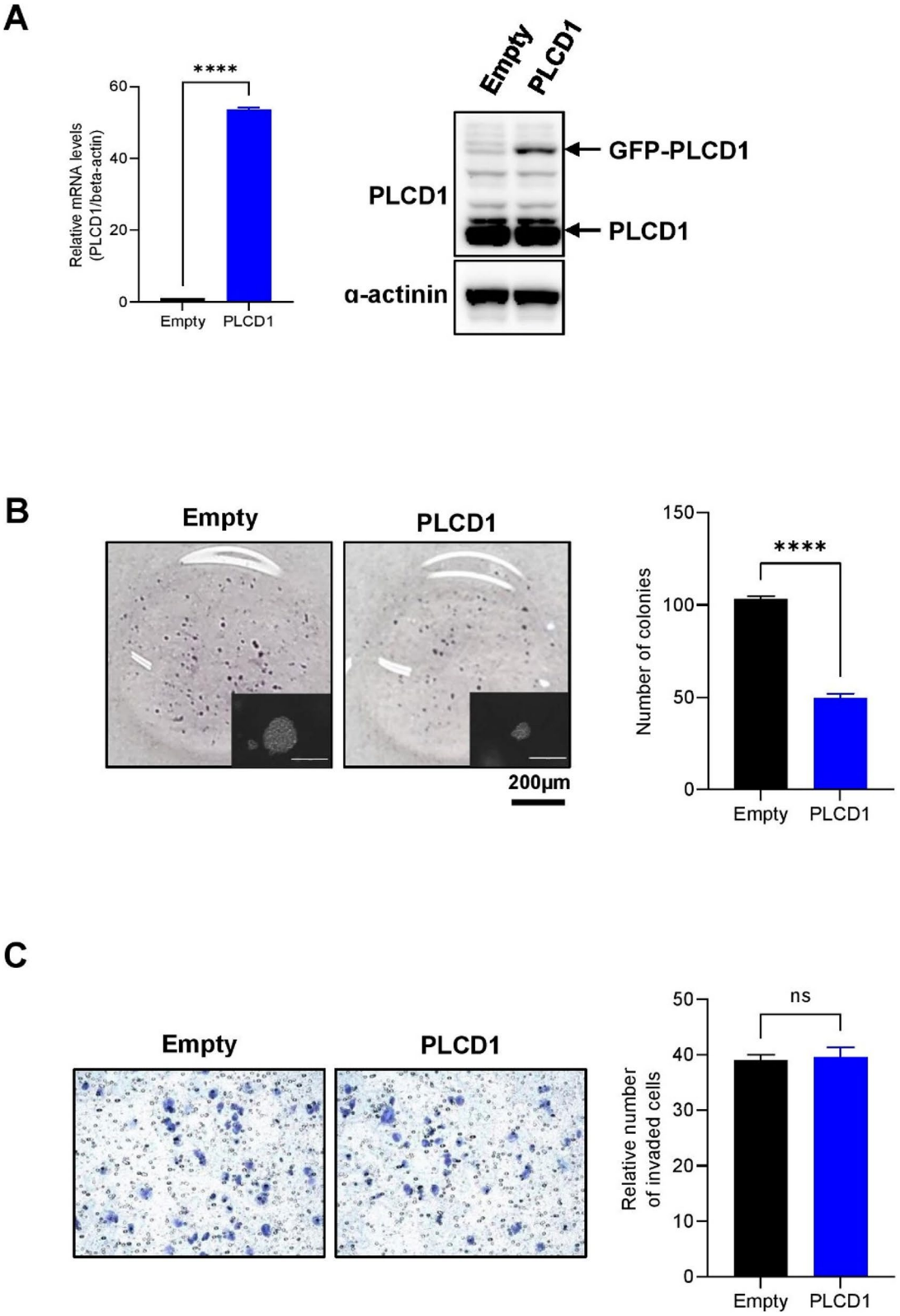

Fig. 3 (See legend on next page.)

(See figure on previous page.)

Fig. 3 PLCD1 overexpression suppressed HGSOC cell proliferation in vitro. (A) OVCAR3 cells were transduced with a GFP-PLCD1 vector or empty control and PLCD1 expression was assessed by Western blotting. PLCD1 and α-actinin lanes were obtained from independent blots performed on different days under identical experimental conditions. α-actinin served as a common loading control across blots. (B) Representative images of spheroids formed from PLCD1-overexpressing and control OVCAR3 cells (scale bar, 200 μm). Spheroids were cultured for 9 days. (C) Invasion assay of OVCAR3 cells transduced with PLCD1 or empty vector. Representative images (left) and quantification of invaded cells (right). Data are shown as mean ± SD (ns: not significant; Mann–Whitney U test)

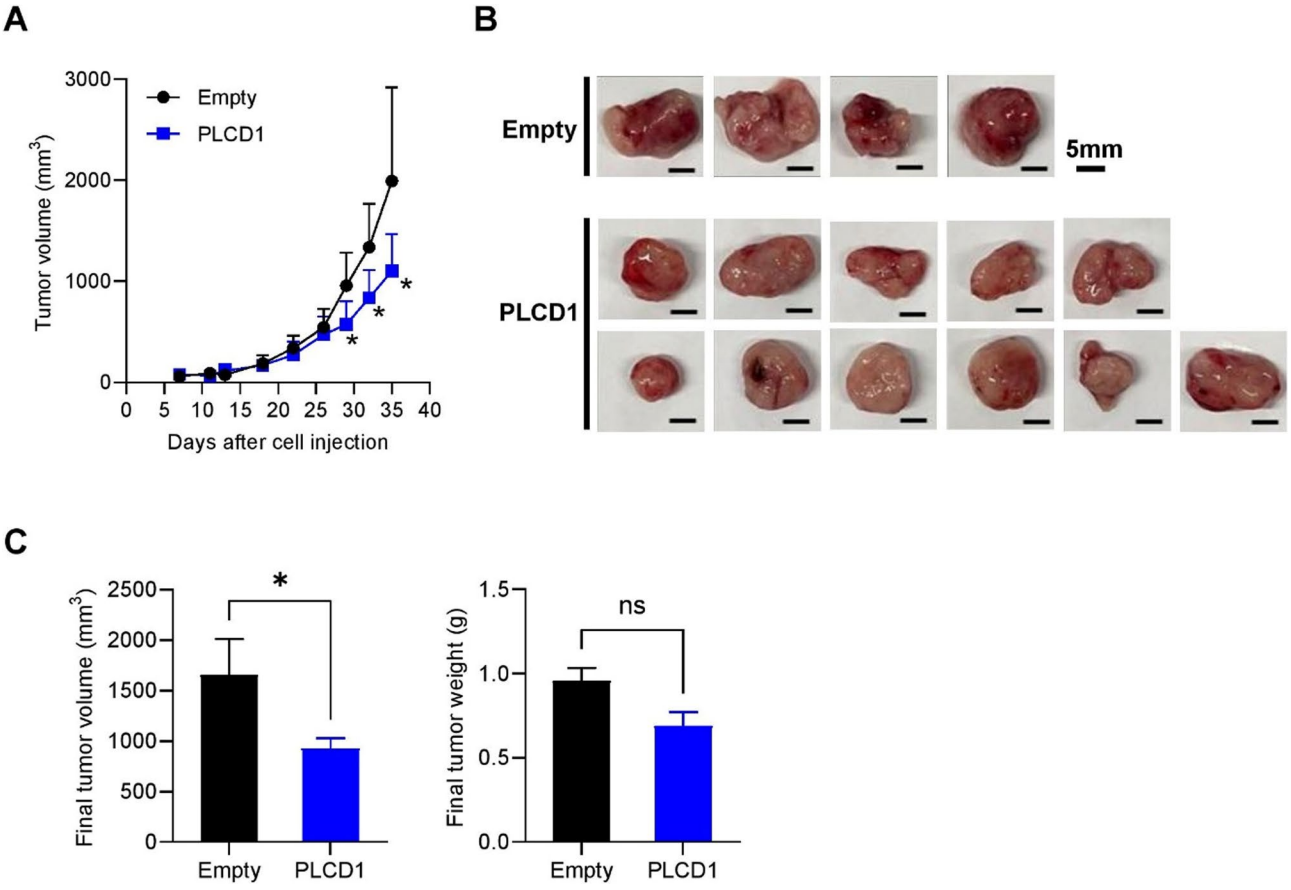

Fig. 4 PLCD1 overexpression inhibited tumor growth in vivo. (A) OVCAR3 cells transduced with either PLCD1 or empty vector were injected subcutaneously into nude mice. Tumor volume was monitored for 35 days. (B) Representative images of tumors on day 35 in the PLCD1 ($n = 11$) and Empty ($n = 4$) groups (scale bar, 5 mm). (C) Final tumor volumes (left) and tumor weights (right) are shown as bar graphs (mean ± SD). Statistical significance was determined using the Mann–Whitney U test ($P < 0.05$; ns: not significant)

with favorable clinical outcomes. While PLCD1 has been reported to be inactivated through promoter methylation in several malignancies, including breast, leukemia, esophageal, and gastric cancer [15–18], its biological role in HGSOC has not previously been characterized. Our data show that PLCD1 expression is significantly higher in HGSOC tissues compared to normal or borderline tissues, suggesting that it may play a role in tumor development and progression. These findings indicate that PLCD1 could serve as a novel marker in HGSOC. In addition, although not statistically significant, we observed a tendency for higher PLCD1 expression in early-stage (I–II) compared with advanced-stage (III–IV) tumors. This trend suggests that PLCD1 upregulation may occur at an early phase of HGSOC, further supporting its potential utility for early detection.

Previous studies have demonstrated that low PLCD1 expression correlates with poor prognosis in various cancers, including renal cell carcinoma, chondrosarcoma, and colorectal cancer [6, 7, 9]. Our results are consistent with these findings, as reduced PLCD1 expression in HGSOC was significantly associated with shorter overall and disease-free survival. To further substantiate

these observations, we analyzed two independent public cohorts (GSE211669 and GSE102073). Consistent with our data, patients with low PLCD1 expression showed significantly shorter OS in GSE211669, and a similar trend was observed in GSE102073 despite not reaching statistical significance. Although PFS outcomes were not statistically significant in either cohort, both datasets showed a tendency toward poorer survival in the low PLCD1 group. Importantly, to our knowledge, this is the first study to demonstrate the prognostic relevance of PLCD1 expression in a gynecologic malignancy. This suggests that PLCD1 may serve as a clinically relevant biomarker in HGSOC, with potential implications for patient stratification and treatment decisions.

To corroborate our in vivo observations, we conducted complementary in vitro studies using two HGSOC cell lines, OVCA429 and OVCAR3. PLCD1 knockdown in OVCA429 cells significantly increased cell proliferation, while PLCD1 overexpression in OVCAR3 cells suppressed cell growth. In addition, xenograft experiments demonstrated that PLCD1 overexpression reduced tumor burden in vivo. Together, these findings suggest that PLCD1 regulates HGSOC cell proliferation in vitro and may contribute to tumor suppression in vivo. Previous studies have reported that PLCD1 is frequently silenced via promoter methylation and exerts tumor-suppressive effects by modulating oncogenic signaling pathways such as WNT/β-catenin and EGFR–FAK–ERK [5, 6]. Additionally, PLCD1 overexpression has been shown to induce DNA damage, resulting in cell cycle arrest and apoptosis [7]. Notably, both WNT/β-catenin and EGFR–FAK–ERK signaling cascades are aberrantly activated in HGSOC and contribute to tumor progression, chemoresistance, and poor prognosis [19, 20], suggesting that PLCD1 may counteract these oncogenic signals. Taken together, these observations support the mechanistic basis of the tumor-suppressive role of PLCD1 in HGSOC. Our study has certain limitations, including the relatively modest sample size of our primary cohort ($n = 101$) and the lack of direct mechanistic validation of the signaling pathways potentially regulated by PLCD1. These aspects were partially addressed through independent GEO cohort analyses and references to mechanistic studies in other malignancies; however, future large-scale clinical cohorts and direct mechanistic investigations are required to validate these interactions.

Collectively, our results support the tumor-suppressive function of PLCD1 in HGSOC and highlight its potential utility as both a diagnostic and prognostic biomarker. Further mechanistic studies are warranted to elucidate the precise pathways through which PLCD1 exerts its effects.

Conclusion

In conclusion, our study provides the first evidence that PLCD1 acts as a tumor suppressor in HGSOC. These findings suggest that PLCD1 may serve as a clinically meaningful biomarker for diagnosis and prognosis, and potentially a therapeutic target in ovarian cancer.

Supplementary Information

The online version contains supplementary material available at https://doi.org/10.1186/s12885-025-15002-1.

Supplementary Material 1.

Supplementary Material 2.

Supplementary Material 3.

Supplementary Material 4.

Supplementary Material 5.

Supplementary Material 6.

Supplementary Material 7.

Supplementary Material 8.

Acknowledgements

Not applicable.

Authors' contributions

Eun-Suk Kang and Jae-Hoon Kim contributed to the study conception and design. Jue Young Kim performed in vitro experiments and analyzed PLCD1 IHC staining results in relation to clinical patient data. Ha-Yeon Shin performed both in vitro and in vivo experiments. Razaul Haque performed TCGA data analysis, prepared the supplementary figures, and contributed to manuscript revision and discussion. Jue Young Kim and Ha-Yeon Shin contributed to clinical sample collection and manuscript preparation. All authors reviewed and commented on previous versions of the manuscript and approved the final version.

Funding

This research was supported by the National Institute of Health (NIH) research project (No. 2024ER051701) and the National Research Foundation of Korea (NRF) grants funded by the Korean government (Ministry of Science and ICT) (RS-2023-00247648, NRF-2022R1F1A1075238, and NRF-2019R1A2C2088715).

Data availability

All data generated or analysed during this study are included in this published article and its supplementary information files.

Ethics approval and consent to participate

This study was approved by the Institutional Review Board of Samsung Medical Center (Approval No. SMC 2019-12-013, approved on December 12, 2019). All patients involved in the study provided written informed consent. TMAs were obtained from the Korea Gynecologic Cancer Bank (KGCB) at Gangnam Severance Hospital, Yonsei University College of Medicine (Approval No. HTB-P2021-5). All experiments involving human participants and human tissue samples were performed in accordance with relevant guidelines and regulations, including the Declaration of Helsinki. All animal experiments were conducted under a protocol approved by the Institutional Animal Care and Use Committee of Yonsei University (IACUC Approval No. 2024 – 0266).

Consent for publication

All authors agree to the publication of this article.

Competing interests

The authors declare no competing interests.

Received: 21 July 2025 / Accepted: 5 September 2025
Published online: 10 November 2025

References

1. Cen Y, Fang Y, Ren Y, Hong S, Lu W, Xu J. Global characterization of extrachromosomal circular DNAs in advanced high grade serous ovarian cancer. Cell Death Dis. 2022;13(4):342.
2. Kim J, Park EY, Kim O, Schilder JM, Coffey DM, Cho CH, et al. Cell origins of high-grade serous ovarian cancer. Cancers (Basel). 2018. https://doi.org/10.3390/cancers10110433.
3. Andrikopoulou A, Theofanakis C, Markellos C, Kaparelou M, Koutsoukos K, Apostolidou K, et al. Optimal time interval between neoadjuvant platinum-based chemotherapy and interval debulking surgery in high-grade serous ovarian cancer. Cancers (Basel). 2023. https://doi.org/10.3390/cancers15133519.
4. Boyarskikh UA, Gulyaeva LF, Avdalyan AM, Kechin AA, Khrapov EA, Lazareva DG, et al. Spectrum of TP53 mutations in BRCA1/2 associated high-grade serous ovarian cancer. Front Oncol. 2020;10:1103.
5. Xie J, Zhou J, Xia J, Zeng Y, Huang G, Zeng W, et al. Phospholipase C delta 1 inhibits WNT/beta-catenin and EGFR-FAK-ERK signaling and is disrupted by promoter CpG methylation in renal cell carcinoma. Clin Epigenetics. 2023;15(1):30.
6. He X, Meng F, Yu ZJ, Zhu XJ, Qin LY, Wu XR, et al. PLCD1 suppressed cellular proliferation, invasion, and migration via inhibition of Wnt/beta-catenin signaling pathway in esophageal squamous cell carcinoma. Dig Dis Sci. 2021;66(2):442–51.
7. Shen J, Yu C, Wang Z, Mu H, Cai Z. PLCD1-Induced DNA damage inhibits the tumor growth via downregulating CDKs in chondrosarcoma. J Oncol. 2022;2022:4488640.
8. Shimozawa M, Anzai S, Satow R, Fukami K. Phospholipase C delta1 negatively regulates autophagy in colorectal cancer cells. Biochem Biophys Res Commun. 2017;488(4):578–83.
9. Xiang Q, He X, Mu J, Mu H, Zhou D, Tang J, et al. The phosphoinositide hydrolase phospholipase C delta1 inhibits epithelial-mesenchymal transition and is silenced in colorectal cancer. J Cell Physiol. 2019;234(8):13906–16.
10. Cho H, Lee YS, Kim J, Chung JY, Kim JH. Overexpression of glucose transporter-1 (GLUT-1) predicts poor prognosis in epithelial ovarian cancer. Cancer Invest. 2013;31(9):607–15.
11. Cho H, Lim BJ, Kang ES, Choi JS, Kim JH. Molecular characterization of a new ovarian cancer cell line, YDOV-151, established from mucinous cystadenocarcinoma. Tohoku J Exp Med. 2009;218(2):129–39.
12. Cho H, Shin HY, Kim S, Kim JS, Chung JY, Chung EJ, et al. The role of S100A14 in epithelial ovarian tumors. Oncotarget. 2014;5(11):3482–96.
13. Garsed DW, Pandey A, Fereday S, Kennedy CJ, Takahashi K, Alsop K, Hamilton PT, Hendley J, Chiew YE, Traficante N, et al. The genomic and immune landscape of long-term survivors of high-grade serous ovarian cancer. Nat Genet. 2022;54(12):1853–64.
14. Ducie J, Dao F, Considine M, Olvera N, Shaw PA, Kurman RJ, Shih IM, Soslow RA, Cope L, Levine DA. Molecular analysis of high-grade serous ovarian carcinoma with and without associated serous tubal intra-epithelial carcinoma. Nat Commun. 2017;8(1):990.
15. Fu L, Qin YR, Xie D, Hu L, Kwong DL, Srivastava G, et al. Characterization of a novel tumor-suppressor gene PLC delta 1 at 3p22 in esophageal squamous cell carcinoma. Cancer Res. 2007;67(22):10720–6.
16. Song JJ, Liu Q, Li Y, Yang ZS, Yang L, Xiang TX, et al. Epigenetic inactivation of PLCD1 in chronic myeloid leukemia. Int J Mol Med. 2012;30(1):179–84.
17. Hu XT, Zhang FB, Fan YC, Shu XS, Wong AH, Zhou W, et al. Phospholipase C delta 1 is a novel 3p22.3 tumor suppressor involved in cytoskeleton organization, with its epigenetic silencing correlated with high-stage gastric cancer. Oncogene. 2009;28(26):2466–75.
18. Xiang T, Li L, Fan Y, Jiang Y, Ying Y, Putti TC, et al. PLCD1 is a functional tumor suppressor inducing G(2)/M arrest and frequently methylated in breast cancer. Cancer Biol Ther. 2010;10(5):520–7.
19. Nagaraj AB, Joseph P, Kovalenko O, Singh S, Armstrong A, Redline R, et al. Critical role of Wnt/beta-catenin signaling in driving epithelial ovarian cancer platinum resistance. Oncotarget. 2015;6(27):23720–34.
20. Zhai X, Shen N, Guo T, Wang J, Xie C, Cao Y, et al. Sptlc2 drives an EGFR-FAK-HBEGF signaling axis to promote ovarian cancer progression. Oncogene. 2025;44(10):679–93.

Publisher's Note